Volume 302, number 3, 256–260 FEBS 11040 May 1992

The polypeptide chain fold in tyrosine phenol-lyase, a pyridoxal-5′-phosphate-dependent enzyme

Alfred A. Antson[a,b], Boris V. Strokopytov[b], Garib N. Murshudov[b], Michail N. Isupov[b], Emil H. Harutyunyan[b], Tatyana V. Demidkina[c], Dmitry G. Vassylyev[c], Zbigniew Dauter[a], Howard Terry[a] and Keith S. Wilson[a]

[a]*European Molecular Biology Laboratory, DESY, Notkestrasse 85, D-2000 Hamburg 52, Germany,* [b]*Institute of Crystallography, Russian Academy of Sciences, Leninsky pr. 59, Moscow 117333, Russia* and [c]*Engelhardt Institute of Molecular Biology, Russian Academy of Sciences, Vavilov str. 32, Moscow 117984, Russia*

Received 30 January 1992; revised version received 3 April 1992

The tyrosine phenol lyase (EC 4.1.99.2) from *Citrobacter intermedius* has been crystallised in the apo form by vapour diffusion. The space group is $P2_12_12$. The unit cell has dimensions a = 76.0 Å, b = 138.3 Å, c = 93.5 Å and it contains two subunits of the tetrameric molecule in the asymmetric unit. Diffraction data for the native enzyme and two heavy atom derivatives have been collected with synchrotron radiation and an image plate scanner. The structure has been solved at 2.7 Å resolution by isomorphous replacement with subsequent modification of the phases by averaging the density around the non-crystallographic symmetry axis. The electron density maps clearly show the relative orientation of the subunits and most of the trace of the polypeptide chain. Each subunit consists of two domains. The topology of the large domain appears to be similar to that of the aminotransferases.

Tyrosine phenol lyase; X-ray analysis; Polypeptide chain fold; Bacterial

1. INTRODUCTION

The different types of modification of amino acids performed by pyridoxal-5′-phosphate (pyridoxal-P)-containing enzymes (including transamination, elimination, decarboxylation and racemisation) have a number of features in common which relate to the mode of binding of coenzyme and substrate molecules and activation of the substrate–enzyme complex. A comparative analysis of the structures of pyridoxal-P-dependent enzymes should provide a better understanding of the relationship between structure and function and show any evolutionary relationship between these enzymes.

To date three-dimensional structures for representatives of three pyridoxal-P-dependent enzymes have been determined, namely a number of aminotransferases from different sources (full references are given in [1]), tryptophan synthase [2], of which the β_2-dimer catalyses the β-replacement reaction, and muscle phosphorylase [3]. Muscle phosphorylase, which clearly is not involved in amino acid metabolism, is not further discussed in this paper.

Tyrosine phenol lyase (TPL) belongs to the group of β-eliminating lyases. The enzyme catalyses the transformation of L-tyrosine to pyruvate, phenol and ammonia [4] and the side transamination reaction [5]. TPL has a molecular weight of about 200 kDa and consists of four identical subunits [6]. Sherman et al. [7] have performed an electron microscopy study of tubular crystals of the enzyme and built a three-dimensional model at 25 Å resolution. Previously we reported the crystallisation and preliminary crystallographic data for TPL [8]. Recently new conditions have been found giving crystals which diffract to higher resolution. The crystallisation, preparation of heavy atom derivatives and solution of the structure at 2.7 Å resolution is described here for these new crystals. A preliminary comparison of the structure with that of other pyridoxal-P-dependent enzymes is presented.

Abbreviations: pyridoxal-P, pyridoxal-5′-phosphate; AspAT, aspartate aminotransferase; TPL, tyrosine phenol lyase.

Correspondence address: A. Antson, European Molecular Biology Laboratory, DESY, Notkestrasse 85, D-2000 Hamburg 52, Germany. Fax: (49) (40) 8908 0149.

2. MATERIALS AND METHODS

A solution of apo TPL was dialysed at 20 mg/ml against 0.1 M potassium phosphate, pH 7.0, with 1 M $(NH_4)_2SO_4$. Crystals were obtained by vapour diffusion against a reservoir containing 0.1 M potassium phosphate, pH 6.0, with 1 M $(NH_4)_2SO_4$. To prepare heavy atom derivatives crystals were first transferred to a 1 M solution of $MgSO_4$ in 0.1 M MES-KOH buffer, pH 6.0. The uranium derivative was prepared by soaking crystals in the same solution containing, in addition, 0.5 mM UO_2SO_4 for 4 days. For the preparation of the mercury derivative crystals were placed in the stabilizing solution with the addition of 0.3 mM $C_2H_5HgH_2PO_4$ for 4 h.

Diffraction data for the native enzyme and heavy atom derivatives were collected, in each case from a single crystal, using synchroton

 Published by Elsevier Science Publishers B.V.

radiation of wavelength in 0.96 Å at the EMBL X11 beam line at the DORIS storage ring, DESY, Hamburg. The rotation method [9] was used with an image plate scanner (J. Hendrix and A. Lentfer, unpublished result) as the detector. Images were processed using a modified version of the MOSFLM program package [10]. Details of the data collection will be published later.

Heavy atom binding sites for the uranium derivative were determined from the difference Patterson synthesis. The mercury derivative was interpreted from the difference Fourier synthesis using phases from the uranium derivative. To improve the phases Bricogne's method of molecular averaging [11] was used with 6 cycles of combination of the isomorphous and calculated phases, followed by 4 cycles of calculation with σ_a weighted [12] $2F_{obs}-F_{calc}$ amplitudes and calculated phases. The position of the non-crystallographic symmetry axis was determined from the self-rotation function and analysis of the coordinates of the heavy atom binding sites. For model building, the program FRODO [13] running on an Evans and Sutherland PS330 interactive graphics station was used. Part of the model was built by the TEK_FRODO program [14]. For refinement of the model the restrained least-squares minimisation program of Konnert and Hendrickson was used [15]. All computations were performed using the CCP4 program package [16].

3. RESULTS

With the conditions described above crystals appeared after 2 weeks and grew to maximum dimensions of 1.0 × 1.3 × 1.3 mm³ after 6–7 weeks. Precession photographs allowed the space group to be identified as $P2_12_12$, the same as for crystallisation at constant pH [8], but with slightly different cell parameters which were now a = 76.0 Å, b = 138.3 Å, c = 93.5 Å. The crystals diffract to 2.3 Å resolution. There are two subunits of the molecule, each with a molecular weight of about 50 kDa, per asymmetric unit of the crystal, giving a specific volume, V_M, of 2.4 Å³ per dalton.

Table I

Summary of map averaging using non-crystallographic symmetry

Number of cycles	Initial *R*-factor	Final *R*-factor	Map averaged
6	0.371	0.294	F_{obs}; combined MIR and calc. phases
4	0.240	0.203	σ_a weighted $2F_{obs}-F_{calc}$; calc. phase

R-factor = $\Sigma|F_{obs}-F_{calc}|/\Sigma F_{obs}$. F_{obs} is the observed structure factor amplitude. F_{calc} and calc. phase are calculated from the averaged density amplitudes and phases. σ_a is defined in [9].

Diffraction data for the native crystal were measured to a resolution of 2.3 Å. The data for the heavy atom derivatives were limited to 2.5 Å for uranium and 3.6 Å for mercury. The value of the merging *R* factors between equivalent measurement of the same reflection (R_1 ($\Sigma|I-\langle I\rangle|/\Sigma I$)·100) for the native, uranium and mercury data were 5.8, 4.6 and 3.5%, respectively.

The successful interpretation of the three-dimensional difference Patterson synthesis for the uranium derivative formed the starting point for the structure determination. Uranium was bound at four sites, one pair related to the other pair by the non-crystallographic symmetry. Nine mercury binding sites were found.

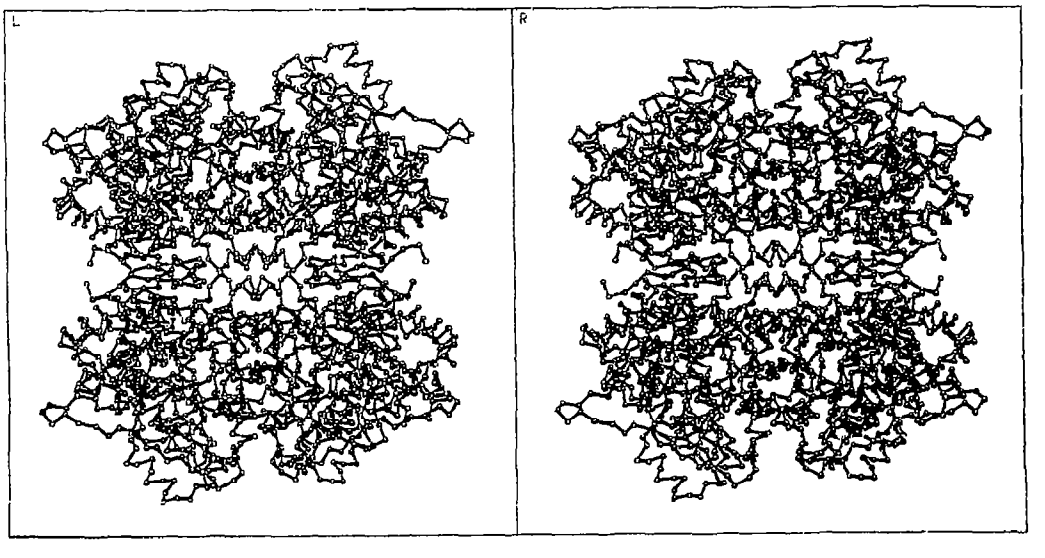

Fig. 1. Stereo view of the C_α backbone of a tetramer of tyrosine phenol lyase.

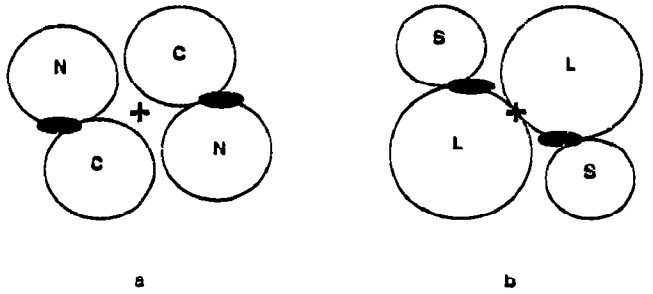

Fig. 2. Schematic representation of the domain architecture: (a) in the β_2-dimer of the $\alpha_2\beta_2$ molecule of tryptophan synthase, and (b) in the dimeric α_2 molecule of AspAT and TPL. Domains are shown as circles and the pyridoxal-P molecules as black lenses. The molecular diads (+) are perpendicular to the picture.

Heavy atom parameters were refined centric reflections only. The resulting Cullis R factor. $R = \Sigma\,||F_{PH} \pm F_P| - F_H|/\Sigma\,|F_{PH} - F_P|$, was 0.53 for the uranium and 0.69 for the mercury derivative. Phases for the protein were calculated at 2.7 Å resolution combining the isomorphous and anomalous signals with a resultant mean figure of merit 0.66.

The point of 222 symmetry of the tetrameric molecule lies at (0; 0.5; 0.777). One of the 2-fold axes is the crystallographic c axis. The two non-crystallographic 2-fold axes make angles of 27° and 117° with the a axis of the unit cell. The statistics of the phase improvement by means of molecular averaging are shown in Table I. The resultant electron density map allowed the tracing of most of the polypeptide chain and the construction of a poly-alanine model in the first instance. When sequence information became available (R.S. Phillips and P. Gollnick, personal communication) the model was rebuilt to incorporate side chains and to correct parts of the main chain. The resulting model contained 85% of the protein atoms. The missing atoms correspond to 4 loops extending into the solvent on the surface of the molecule. This model was subjected to 10 cycles of refinement, and the R factor is currently 27.6% for data between 10.0 Å and 2.7 Å resolution.

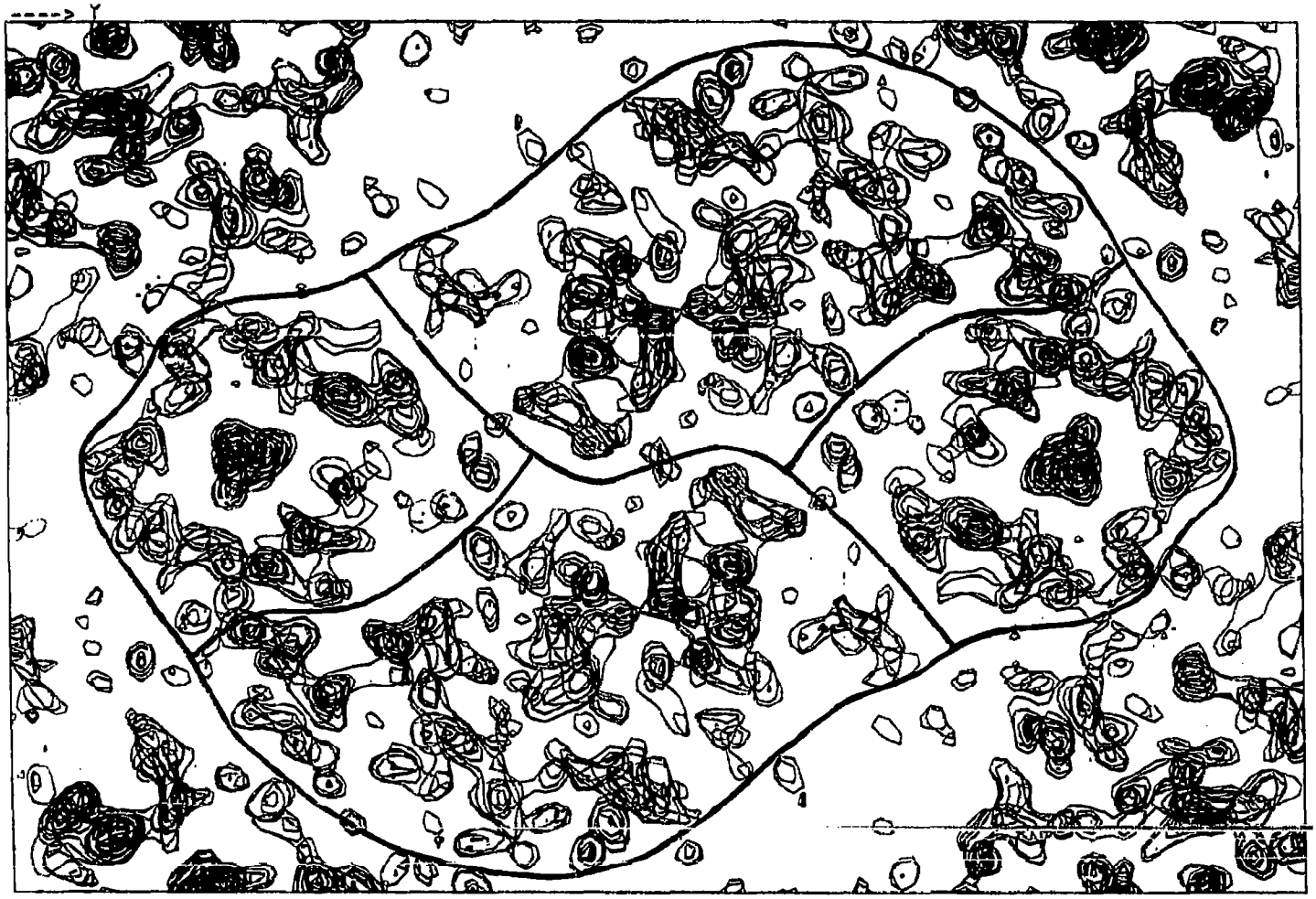

Fig. 3. Ten superimposed sections of the electron density map showing the arrangement of the domains in two subunits related by the crystallographic 2-fold axis. The crystallographic two-fold axis is at the centre, perpendicular to the plane of the figure.

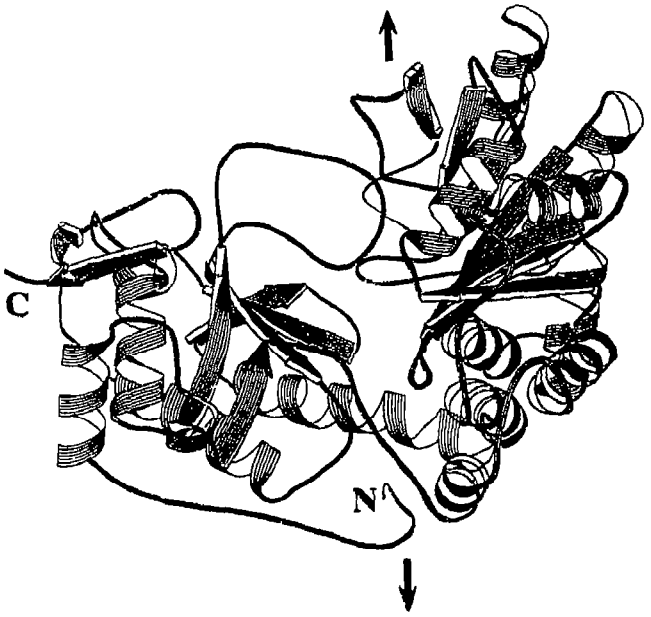

Fig. 4. A ribbon model of the TPL subunit. The large domain is on the right and the small on the left of the figure. Position of the crystallographic 2-fold axis is marked.

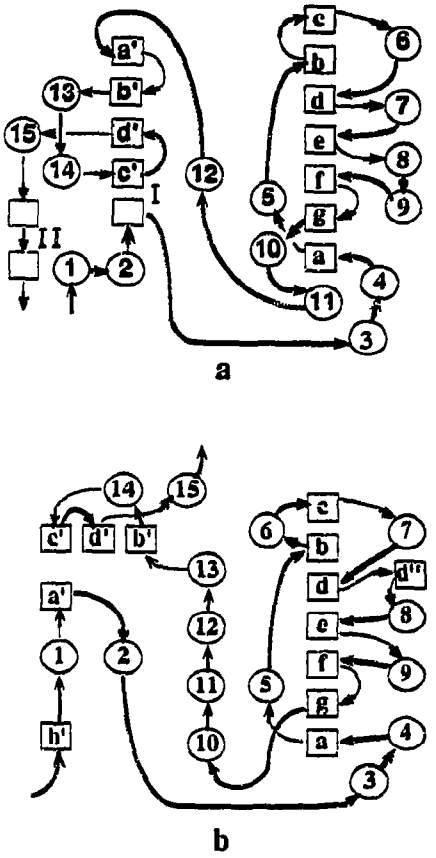

Fig. 5. Topology diagrams of (a) TPL and (b) AspAT [16] subunits. The β-strands are represented as squares and the α-helices as circles. The view is comparable to that in Fig. 4.

4. DISCUSSION

The relative arrangement of the subunits in the α_4 TPL tetramer is shown in Fig. 1, with the crystallographic 2-fold axis vertical. There are fewer intersubunit contacts across the non-crystallographic 2-fold axis than across the crystallographic 2-fold axis. Thus the tetramer appears to be built up of two dimers with weaker contacts than between the monomers in a dimer. Each polypeptide chain is folded into small and large domains.

There are two different types of domain architecture found in pyridoxal-P-dependent enzymes up to now. One is that in the β_2-dimer of the $\alpha_2\beta_2$ tryptophan synthase complex [2], Fig. 2a. Each subunit consists of two domains, almost equal to each other in size, labelled as N and C (N-terminal and C-terminal, respectively). The coenzyme molecule is located between two domains and the second subunit seems not to contribute to the active site of the first. The other type of architecture is that first found in the α_2 molecule of mitochondrial aspartate aminotransferase (AspAT) [17], where the domains differ in size. They are marked as L and S (large and small) in Fig. 2b. Here each active site of the dimeric molecule is composed of amino acid residues from both the large and small domains of one subunit and the large domain of the neighbouring subunit, and the pyridoxal-P moiety is located at this interface.

Fig. 3 shows several superimposed sections of the TPL electron density map with indication of the boundaries of the domains in the two subunits, related by a crystallographic 2-fold axis. The domain architecture in that dimer is clearly analogous to that in the AspAT molecule. Assuming that the coenzyme moiety is located in the hole between the large and the small domains, as in AspAT, then the active site in each subunit of TPL involves residues from the large domain of another subunit, symmetry-related by the crystallographic 2-fold axis.

The ribbon model [18] of a single subunit of TPL is shown in Fig. 4, and the topology diagram vs. that of AspAT [19] in Fig. 5. Each subunit of the TPL molecule can be divided into three parts: (i) a small domain which consists of the N- and C-terminal parts of the polypeptide chain (amino acids 20–48, 333–456); (ii) a large domain comprising the central part of the chain (amino acids 57–310); (iii) the two pieces of chain connecting the two domains. The core of the small domain is made up of a four-stranded antiparallel β-sheet. Seven β-strands form a β-sheet of mixed type in the core of the large domain. Almost all of the α-helices are located on the surface of the subunit. The connection from the large to the small domain includes α-helix 12, the longest helix in TPL comprising 20 amino acids.

The main differences between the structure of TPL and AspAT are in the small domains. In both proteins

the core of the large domain is formed by a β-sheet with the same β-strand topology. The positions of the α-helices around the β-sheet are also quite similar. The connection from the large to the small domain in both cases is formed by the longest α-helix in the structure. Thus, AspAT and TPL appear to have similar topology in the large domain and similar quaternary structures, different from that found in tryptophan synthase. Detailed comparison and analysis of the TPL active site must await the refined high resolution structure of TPL. A full description of the structure analysis and refinement will be published later.

Acknowledgements: We thank Robert S. Phillips and Paul Gollnick for giving us the sequence of TPL in advance of publication. We are grateful to Hidehiko Kumagai for providing us with the cells of *Citrobacter intermedius*. A.A.A. thanks FEBS for a fellowship in supporting this work in EMBL, Hamburg.

REFERENCES

[1] Fukui, T., Kagamiyama, H., Soda, K. and Wada, H. (1991) Enzymes dependent on pyridoxal phosphate and other carbonyl compounds as cofactors, part II, Pergamon Press, Oxford.
[2] Hyde, C.C., Ahmed, S.A., Padlan, E.A., Miles, E.W. and Davies, D.R. (1988) J. Biol. Chem. 263, 17857–17871.
[3] Barford, D. and Johnson, L.N. (1989) Nature 340, 609–616.
[4] Kumagai, H., Yamada, H., Matsui, H., Ohkishi, H. and Ogata, K. (1970) J. Biol. Chem. 245, 1767–1772.
[5] Demidkina, T.V. and Myagkikh, I.V. (1989) Biochimie 71, 565–571.
[6] Kuzakov, V.K., Tarusina, I.I., Myagkikh, I.V. and Demidkina, T.V. (1987) Biokhimia 52, 1319–1323 (Russian).
[7] Sherman, M.B., Antson, A.A., Orlova, E.V., Zograf, O.N. and Demidkina, T.V. (1990) Dokl. Akad. Nauk USSR 312, 1256–1258 (Russian).
[8] Demidkina, T.V., Myagkikh, I.V., Antson, A.A. and Harutyunyan, E.H. (1988) FEBS Lett. 232, 381–382.
[9] Arndt, U.W. and Wonacott, A.J. (1977) The Rotation Method in Crystallography, Elsevier, Amsterdam.
[10] Leslie, A.G.W., Brick, P. and Wonacott, A.J. (1986) CCP4 News 18, 33–39.
[10] Leslie, A.G.W., Brick, P. and Wonacott, A.J. (1986) CCP4 News 18, 33–39.
[11] Bricogne, G. (1976) Acta Crystallogr. A32, 832–847.
[12] Read, R.G. (1986) Acta Crystallogr. A42, 140–149.
[13] Jones, T.A. (1978) J. Appl. Crystallogr. 11, 268–272.
[14] Vassylyev, D.G. and Adzubei, A.A. (1992) J. Mol. Graphics (in press).
[15] Konnert, J.H. and Hendrickson, W.A. (1980) Acta Crystallogr. A34, 791–809.
[16] CCP4 (1979) The SERC (UK) Collaborative Computing Project No. 4. A suite of programs for protein crystallography, distributed from Daresbury Laboratory, Warrington, England.
[17] Ford, G.C., Eichele, G. and Jansonius, J.N. (1980) Proc. Natl. Acad. Sci. USA 77, 2559–2563.
[18] Priestle, J. (1988) J. Appl. Crystallogr. 21, 572–576.
[19] Harutyunyan, E.G., Malashkevich, V.N., Tersyan, S.S., Kochkina, V.M., Torchinsky, Yu.M. and Braunstein, A.E. (1982) FEBS Lett. 138, 113–116.